NIH Public Access
Author Manuscript
J Control Release. Author manuscript; available in PMC 2014 November 10.

Published in final edited form as:
J Control Release. 2013 November 10; 171(3): 288–295. doi:10.1016/j.jconrel.2013.06.023.

Proteolytically activated anti-bacterial hydrogel microspheres

Jason S. Buhrman[1], **Laura C. Cook**[2], **Jamie E. Rayahin**[1], **Michael J. Federle**[2], and **Richard A. Gemeinhart**[1,3,4,*]

[1]Department of Biopharmaceutical Sciences, University of Illinois, Chicago, IL 60612-7231, USA.

[2]Center for Pharmaceutical Biotechnology, Department of Medicinal Chemistry and Pharmacognosy, University of Illinois, Chicago, IL 60607-7173, USA.

[3]Department of Bioengineering, University of Illinois, Chicago, IL 60607-7052, USA.

[4]Department of Ophthalmology and Visual Sciences, University of Illinois, Chicago, IL 60612-4319, USA.

Abstract

Hydrogels are finding increased clinical utility as advances continue to exploit their favorable material properties. Hydrogels can be adapted for many applications, including surface coatings and drug delivery. Anti-infectious surfaces and delivery systems that actively destroy invading organisms are alternative ways to exploit the favorable material properties offered by hydrogels. Sterilization techniques are commonly employed to ensure the materials are non-infectious upon placement, but sterilization is not absolute and infections are still expected. Natural, anti-bacterial proteins have been discovered which have the potential to act as anti-infectious agents; however, the proteins are toxic and need localized release to have therapeutic efficacy without toxicity. In these studies, we explore the use of the glutathione s-transferase (GST) to anchor the bactericidal peptide, melittin, to the surface of poly(ethylene glycol) diacrylate (PEGDA) hydrogel microspheres. We show that therapeutic levels of protein can be anchored to the surface of the microspheres using the GST anchor. We compared the therapeutic efficacy of recombinant melittin released from PEGDA microspheres to melittin. We found that, when released by an activating enzyme, thrombin, recombinant melittin efficiently inhibits growth of the pathogenic bacterium *Streptococcus pyogenes* as effectively as melittin created by solid phase peptide synthesis. We conclude that a GST protein anchor can be used to immobilize functional protein to PEGDA microspheres and the protein will remain immobilized under physiological conditions until the protein is enzymatically released.

Keywords

recombinant protein; glutathione s-transferase; glutathione; thrombin; hydrogel; microparticles

© 2013 Elsevier B.V. All rights reserved.

[*]**Correspondence to:** Richard A. Gemeinhart, 833 South Wood Street (MC865), Chicago, IL 60612-7231, USA. rag@uic.edu.

Publisher's Disclaimer: This is a PDF file of an unedited manuscript that has been accepted for publication. As a service to our customers we are providing this early version of the manuscript. The manuscript will undergo copyediting, typesetting, and review of the resulting proof before it is published in its final citable form. Please note that during the production process errors may be discovered which could affect the content, and all legal disclaimers that apply to the journal pertain.

NIH-PA Author Manuscript
NIH-PA Author Manuscript
NIH-PA Author Manuscript

NIH-PA Author Manuscript
NIH-PA Author Manuscript
NIH-PA Author Manuscript

1.0 Introduction

Most modern advances in medical technology put sterility as a first point in design principles. Conventionally, these systems are passively sterilized to prevent infection before they are used. Being an incomplete process, materials implanted or inserted into the body are expected to have an incidence of infection with even the best methods of sterilization. Nosocomial infections from passively sterilized materials, *e.g.* catheters, artificial joints, pacemakers and drug pumps, cause more than 1.5 million deaths each year [1–3]. Therefore, methods beyond passive sterilization are necessary. Active anti-infectious materials are thought to be superior to the currently used, passively sterilized, noninfectious materials in maintaining sterility in non-sterile environments.

Recent reports of actively anti-infectious systems are emerging. These systems include the use of charged polymers that interact with membranes of bacteria [4], nitric oxide coatings [5], antibiotic coatings [6], silver coatings [7], and antibody coatings [8] (reviewed in [9]). These systems have been shown to actively inhibit the growth of invasive bacteria and reduce the risk of infection. Local delivery of anti-bacterial therapy has been achieved by polymeric microspheres [10–12]. Further improvements are necessary to limit local infections.

Hydrogels are becoming more prevalent in medical use as delivery systems [13, 14], implants [14], drug excipients [14, 15], and coatings [16]. Hydrogels are highly adaptable and have the potential as a platform for modifying other mateirals. In this report, we describe a microsphere-based, active antibacterial hydrogel delivery system. The hydrogel microsphere system is, to our knowledge, the first activated by the local immune response to bacterial infection into releasing an anti-bacterial compound. The system utilizes the tripeptide glutathione (GSH), a highly versatile molecule readily attachable to most surfaces. GSH was immobilized onto poly(ethylene glycol) diacrylate (PEGDA) hydrogel microspheres to allow for a modular system of anchoring therapeutic glutathione s-transferase (GST) fusion proteins. The GSH-GST interaction has long found utility in recombinant protein technology [17] but not in drug delivery to date.

Here, we present data that GST fusion proteins may be bound to GSH-laden microspheres. To deliver specific proteins during infection, thrombin-cleavable sites were engineered in the junction between GST and the fused protein to serve as an activation site. Upon thrombin cleavage, the target protein dissociates from the immobilized GST. Microspheres with GST attached to green fluorescent protein (GFP) were made as a control to demonstrate proper formation of the complex and proper release by thrombin (Fig. 1A).

As a model anti-bacterial therapeutic, melittin was attached to microspheres to act as a lytic peptide against bacterial pathogens [19–21] following cleavage. Thrombin cleavage was chosen due to the fact that thrombin is activated by the host immune system at sites of inflammation caused by bacterial pathogens, such as the Gram-positive bacterium *Streptococcus pyogenes*, among others [22]. Both the therapeutic molecule and protease are models and can be readily altered in this platform. GSH-laden PEGDA hydrogel microspheres, thus, can interact with GST-fused proteins and act as a delivery system for antibacterial proteins or peptides, such as melittin. It is reasoned that proteolysis by host-derived thrombin at sites of infection will facilitate release of melittin and subsequently, the killing of pathogenic bacteria.

NIH-PA Author Manuscript

NIH-PA Author Manuscript

NIH-PA Author Manuscript

2.0 Materials and Methods

2.1 Expression and purification of recombinant proteins

Proteins were expressed and purified by methods previously reported [23]. In brief, GFP was cloned from the pWiz-GFP plasmid (Aldevron, Madison, WI) into the pGex-6p-1 plasmid (GE healthcare, Waukesha, WI) by primer extension PCR. A hexa-histidine tag and thrombin cleavage site (LVPRGS) were added to the N-terminal of GFP prior to insertion, generating pJB-HTS-GFP [24]. Melittin (GIGAVLKVLTTGLPALISWIKRKRQ) [19, 20] was codon optimized using JCAT [25]: (AGC *GGA TCC* GGT ATC GGT GCT GTT CTG AAA GTT CTG ACC ACC GGT CTG CCG GCT CTG ATC TCT TGG ATC AAA CGT AAA CGT CAG TAG ***GAATTC*** TCA CG) and cloned into the same vector replacing GFP after removal by BamHI and EcoRI (NEB, Cambridge, MA) generating pJB-HTS-melittin [23].

Proteins were expressed in BL21 and Rosetta (Novagen/EMD Millipore, Billerica, MA) *Escherichia coli* cells for GST-GFP and GST-melittin, respectively. In both cases, bacterial cells were grown to an absorbance at 600 nm (A_{600}) of 0.4 at 37°C before addition of 0.1 mM IPTG [24] to induce protein production. Cells were removed to 25°C and incubated for 16 hours to produce the fusion proteins. Bacterial cells were centrifuged before re-suspension in lysis buffer (50 mM $NaHPO_4$, 300 mM NaCl, buffered to pH 8.0). Cells were lysed by three freeze-thaw cycles on dry ice and 4°C before three 15-second sonication (Misonix model XL2015) rounds at 40% intensity with 15-second incubation on ice between sonication rounds. The lysate was centrifuged at 12,000 RPM and 4°C for 30 minutes to pellet the insoluble material. GST-GFP was predominantly in the soluble fraction and was purified by Ni-NTA chromatography (Qiagen, Germantown, MA) according to the manufacturer's recommendation. GST-melittin was predominantly in the insoluble fraction and was extracted by 1% Tween-20. The extract was then purified by Ni-NTA chromatography yielding a column elution product determined to be approximately 50% GST, 50% GST-melittin.

2.2 PEGDA microsphere formation, protein loading, and characterization

All chemicals are from Thermo Fisher Scientific (Waltham, MA) unless otherwise noted. PEGDA microspheres were created through a modified process of reverse phase emulsion polymerization [24, 26]. PEGDA (300 μL; MW = 575 g/mol, Sigma-Aldrich, St. Louis, MO) was diluted in 300 μL PBS containing 30 mg reduced glutathione (GSH) or 12 mg (equimolar with GSH) reduced cysteine (Sigma-Aldrich, St. Louis, MO). The microspheres made in the presence of glutathione and cysteine are referred to as PEGDA-GSH and PEGDA-cys, respectively. Mineral oil (2 mL) was added to a borosilicate culture tube (1.5 mm diameter, 10 mm length). Monomer solution (100 μL) was added to the culture tube while vortexing for 10 seconds at full speed. While still vortexing, 100 μL of 20% ammonium persulfate (in PBS) was added followed by 50 μL N,N,N',N'-tetramethyl ethylene diamine. The mixture was vortexed for an additional minute. Deionized water (2 mL) was added prior to centrifugation at 4°C, 4,000 rpm for 1 minute to recover the microspheres. Microspheres were washed over the course of a week at 4°C with greater than a 10-fold volume of PBS and with 5 to 10 changes of PBS per day. Microspheres were loaded over the course of 3 hours with 50 to 100 μg of protein in PBS. Loading occurred on a rotator wheel, with gentle rotation at 20 RPM. After loading, microspheres were washed one time with 10-fold excess volume of PBS.

Microscopy was carried out on an Olympus IX70 inverted microscope with an epifluorescent illuminator. Images were captured by a Q-imaging Retiga 1300 CCD and analyzed on Q-capture suite. The diameter of at least 130 particles was measured from at

NIH-PA Author Manuscript

NIH-PA Author Manuscript

NIH-PA Author Manuscript

least three different particle preparations for each formulation. Fluorescent images are pseudocolor micrographs using the fluorescent properties of GFP (excitation and emission: 488 and 519 nm) or trypan blue (excitation and emission: 595 and 660 nm) [27–29]. To determine particle density in solution PEGDA microspheres were counted using hemocytometer after staining with trypan blue (1% in PBS).

Mesh size of macroscopic hydrogels formed using identical conditions without emulsification was measured as previously described [30–32]. Briefly, after polymerization in an 8 mm × 2 mm cylindrical mold, polymers were suspended in 1-butanol and the mass of butanol displaced by the suspended polymer was noted. Hydrogels were swollen over twenty-four hours in deionized water, and their masses recorded. The hydrogels were returned to water and masses recorded at three-hour intervals until there was a difference between subsequent masses of less than 5%, deemed equilibrium swelling. At this point, the swollen hydrogels were re-suspended in butanol and the mass of butanol displaced by the suspended polymer was determined. Hydrogels were then freeze-dried for 24 hours, and their dry weight recorded. Mesh size were estimated based upon the Flory-Rehner swelling theory [33].

2.3 Protein Identity, Quantitation, and Kinetics

Total protein was determined by the Bradford Assay (Pierce) [34] according to the manufacturer recommendations and measured with a Beckman model DU640 spectrophotometer. Acrylamide gels were prepared in house by conventional protocols [35]. All gels were between 12% and 15% acrylamide and crosslinked at a ratio of 37.5 to 1 acrylamide to bis-acrylamide. Gels were stained by Coomassie brilliant blue. Images were captured on a light table with a Sony DSC-H9 cybershot CCD.

Reaction kinetics were measured by semi-quantitative densitometry of SDS-PAGE gels and fluorometry. Reactions with equivalent concentrations of GST-GFP substrate and varying concentrations of thrombin (0.1, 0.33, 0.75, 1.5, and 3 μM) were incubated at 37°C for varying amounts of time. In groups where cleavage from microspheres is reported, approximately 10,000 microspheres were used. Reactions for densitometry were stopped by addition of Laemmli sample buffer [36] (containing SDS) and stored at 4°C until run on SDS-PAGE. Reactions for fluorometry were stopped by addition 1 mM phenyl methyl sulfonyl fluoride (PMSF) and immediately read on a Turner Quantech Fluorometer (Cole Parmer, Vernon Hills, IL). The excitation filter was a band pass 490 nm and the emission filter was long pass 550 nm. All gels were run with known concentrations of BSA standards. Density measurements were made with NIH imageJ software with gel backgrounds normalized. Each thrombin concentration was run one time, except for 0.73 μM, which was run in biological triplicate.

2.4 Protein Release

GSH mediated release studies were carried out over 6 days. Protein release was measured from 10,000 to 20,000 microspheres into 500 μL PBS in the presence absence of glutathione. Release was measured with three independent replicates per experimental group. Preliminary studies (not shown) indicated that in this system, 50% of reduced glutathione becomes oxidized within 24 hours. Therefore, at each 24-hour time point, glutathione containing buffers were completely replaced. Removed buffer was frozen for later analysis. At the completion of the experiment, all frozen samples were thawed and 50 μL of each samples were diluted in PBS and read on a Quantech fluorometer.

Anti-coagulated (citrate) human plasma (Innovative Research, Novi, MI) from three different donors was incubated with microspheres at 37°C for six days. Plasma (100 μL) was

NIH-PA Author Manuscript

NIH-PA Author Manuscript

NIH-PA Author Manuscript

incubated in a 96-well plate in the presence of PEGDA-GSH microspheres anchoring GST-GFP. At the end of six days, photographs were taken of the wells, and fluorescence was measured in the plasma supernatant. The University of Illinois at Chicago Institutional Review Board approved the study protocol for use of human plasma.

2.5 S. pyogenes growth inhibition

In a volume of 500 μL, approximately two million PEGDA-GSH microspheres were loaded with GST-melittin over a period of three hours. The microspheres were washed with 10 times volume of PBS one time, and divided into two tubes. Thrombin (2U) was added to one tube containing one-million GST-melittin loaded microspheres, and two additional units of thrombin were loaded to a third tube containing one-million PEGDA-GSH microspheres that were not loaded with GST-melittin. Samples were incubated at 37°C for two hours before the supernatant was removed.

S. pyogenes cells were grown in Todd Hewitt broth (Becton Dickenson) supplemented with 0.5% yeast extract. Following overnight growth, cells were diluted 1:100 into chemically defined medium [37] to a final concentration of ~10^7 colony forming units/mL. Supernatant (50 μL) of washed spheres was added to 400 μL of cells. Each sample (50 μL) was added, in triplicate wells, to a 96-well optical bottom plates (Greiner BioOne). This plate was incubated at 37°C for twelve hours while shaking. At ten-minute intervals, the absorbance at a wavelength of 600 nm (A_{600}) was recorded (Biotek Synergy 2 spectrophotometer; Winooski, VT).

2.6 Statistical Analysis

ANOVA was used to test all groups, and post-hoc Tukey analysis was utilized for pairwise comparison if ANOVA suggested significant differences between the groups. In all cases α less than or equal to 0.05 was considered significant.

3.0 Results

GST is encoded as a monomer, but forms a dimer in the native state in solution [38, 39]. The dimer has been crystalized in its dimeric form [40] as has the GFP protein [41]. Using this information and structure predictions [18], estimates for the size of fusion proteins (Fig. 1B). Monomeric and dimeric GSH fusion proteins (Table 1) were determined. To predict if proteins of these dimension would enter the hydrogels, we measured the mesh size (ξ) of the PEGDA-GST hydrogels to be 4.6±0.2 nm. The addition of 5 to 1 molar ratio of PEGDA to GSH did not significantly affect mesh size from the PEGDA hydrogels without GSH, which had a mesh size of 4.5±0.1 nm. Based upon estimates of fusion protein size and the mesh size, GST monomers or dimers would be unlikely to enter the hydrogel mesh even without being fused to another protein. To further support this, PEGDA-GSH microspheres were loaded with GST-GFP and nonspecifically stained with trypan blue to allow localization of the protein. Microspheres visualized by epifluorescent microscopy exhibited GFP (green) predominantly on their surface while trypan blue (red) was observed throughout the microspheres in a diffuse pattern (Fig. 2). We concluded that the interaction between GST-GFP and PEGDA-GSH microspheres was occurring predominantly at surface of the microspheres.

Assuming that the entire surface of a PEGDA microsphere was available for interaction with GST-GFP, we calculated the number of GST-GFP that could bind to the surface assuming perfect, monolayer coverage. Hydrogel microspheres had an average diameter of 46±16 μm (Fig. 3, Table 2). Using individual microsphere diameter, the average surface area of an average sphere was calculated to be 6,647±804 μm^2 (Table 2) after synthesis, washing, and

NIH-PA Author Manuscript

NIH-PA Author Manuscript

NIH-PA Author Manuscript

loading with GST-GFP. Measurements on control PEGDA-cysteine (cys) microspheres showed similar size and surface area distributions (Fig. 3). Assuming an ellipsoid projection of the dimeric GST-GFP or GST-melittin with binding in the pocket on the x-y plane (Fig. 1B, **left**), we reasoned that the binding area of a GST fusion protein molecule, either GST-GFP or GST-melittin, to be 1.4×10^{-5} μm^2 (Fig. 1B, **right**). Given these values and the assumption that all GST-GFP loading is on the surface, we predicted that monolayer coverage of an average PEGDA-GSH microsphere would consist of 4.7×10^8 molecules of GST-GFP or GST-melittin.

With the estimate of the amount of protein loaded on the microspheres, the ability to release the protein in a specific manner was assessed. PEGDA-GSH and PEGDA-cys microspheres were first loaded for three hours with GST-GFP. PEGDA-cys microspheres are used, in this case, as a control for non-specific binding and release of protein. When placed in buffer, PEGDA-cys microspheres released 0.98±0.4 μg of GFP in 6 days, but PEGDA-GSH microspheres released no measurable GFP in this period. Although the washing of PEGDA-cys microspheres was not complete and some surface binding of the fusion protein was detected ($1.82 \pm 1.1 \times 10^8$ molecules per microsphere), this was rapidly released from microspheres without need for protease or glutathione. For the PEGDA-GSH microspheres, that did not elute any detectable GFP in 6 days, thrombin was able to cleave $9.9 \pm 2.5 \times 10^8$ molecules of GFP per PEGDA-GSH microsphere. Based upon this result, GST-GFP bound to PEGDA-GSH microspheres represents significantly more than monolayer coverage. And it is clear that the interaction between GST fusion proteins and the PEGDA-GSH microspheres is specific.

To further confirm the specificity of the interactions of GST-GFP with the surface and to give a preliminary understanding of the expected response of the microspheres following injection into extracellular fluids, we examined the release of protein from microspheres in the presence of free GSH. GSH is available at low levels (0.1 mM) in extracellular compartments of the body [43]. Extracellular GSH will elute proteins immobilized by GST/GSH interactions, but based upon the knowledge of the association constant, K_m, between GSH and GST (2.2×10^{-2} mM) [44], the elution of GST-GFP protein anchored to PEGDA-GSH microspheres was expected to be low. Over a period of time, GST-GFP elution was measured in buffer containing various GSH concentrations. GSH at intracellular levels (10 mM and 1mM) eluted a significant portion GST-GFP within 48 hours. Extracellular levels of GSH, *i.e.* concentrations below 1 mM GSH had a much less prominent disruption of the microsphere GST-GFP interaction with more than 80% of the protein remaining associated with the particles after 6 days (Fig. 4A).

To further understand the strength of the interaction in complex biologic fluids, we challenged PEGDA-GSH microspheres anchoring GST-GFP with anti-coagulated human plasma for six days at 37°C. We found that after six days almost no GFP was released into the plasma (Fig. 4B), and the microspheres remained brightly fluorescent suggesting the bound protein was still active (Fig. 4C). Protein is clearly not released from the microspheres without the presence of proteases in the fluid. Although plasma does not contain many blood proteases in the active form due to calcium depletion, the small molecules, ions, and active proteases in citrated plasma do not release proteins significantly. Because many plasma proteases, including prothrombin, become activated by blood draw, addition of calcium can be used to achieve active proteolytic plasma, but this activated plasma has significantly higher protease activity than plasma before the blood draw [45–47].

With an understanding that the association is specific, we sought to determine the release in the presence of physiologic thrombin concentrations. Compared with the absence of thrombin (Fig. 4A), significantly faster GFP release was observed when thrombin mediated

NIH-PA Author Manuscript

NIH-PA Author Manuscript

NIH-PA Author Manuscript

the release (Fig. 5A). Protein was released on a time scale of minutes compared to days when no enzymatic response was present. Microscopy clearly demonstrates the release of GFP from GST-GFP loaded PEGDA-GSH microspheres following thrombin exposure (Fig. 5B). By comparing the rate of GST-GFP cleavage between free GST-GFP and PEGDA-GSH associated GST-GFP, the rate of cleavage was significantly higher for free (unbound) GST-GPF compared to bound GST-GPF at all concentrations of thrombin (Fig 5C). This would be expected since the orientation and mobility of the substrate would be restricted resulting in diminished binding of thrombin and possibly restricted cleavage due to the orientation of the molecules.

To determine the effectiveness of the GSH-GST interaction as a thrombin mediated, anti-bacterial delivery system, we generated GST-melittin and loaded this protein on PEGDA-GSH microspheres in a manner equivalent to the GST-GFP protein. GST-melittin binds to PEGDA-GSH microspheres similarly to GST-GFP with an estimated 7.8±1.5 molecules of melittin per microsphere. This is not significantly different (p-value greater than 0.05) from the number of GFP molecules estimated to be present on the surface of PEGDA-GSH microspheres, 9.9±1.3 molecules per microsphere. Following exposure of these GST-melittin loaded microspheres to thrombin, the released protein, or appropriate controls, was incubated with *S. pyogenes* cells. GST-melittin loaded microspheres that had been activated with thrombin inhibited *S. pyogenes* growth similarly to 10 μM synthetic melittin over a period of 12 hours. Protein released from microspheres without thrombin treatment had a limited growth inhibition (Fig. 6).

4.0 Discussion

We chose to conduct these studies with PEGDA as the base for the hydrogels because PEGDA is an FDA approvable material already in use in clinics [48]. Hydrogels can be surface-modified [49] or layered onto various surfaces with the potential for controlling cellular interactions and for drug delivery [50–54]. We also chose PEGDA as the polymer du to the thiol-ene addition of GSH to PEGDA in a single step [55]. Although the system is developed with PEGDA, this approach is easily amendable to nearly any hydrogel system, and possibly beyond hydrogel systems. Hydrogel microspheres were utilized because of the increased surface to volume ratio allowed high binding capacity the potential for clinical application as locally injected systems [56–58].

One property of hydrogels that can be modulated is the mesh size. In our current system, the mesh size of the hydrogel microspheres limited proteins from entering the microspheres. Based upon our past experience with PEGDA hydrogels [13, 30, 59], we designed the hydrogel to have a mesh that would exclude the GST fusion proteins from the interior of the microspheres. The calculated mesh size agreed with this design prediction. From the measurements of the size of the microspheres, a monolayer of dimeric GST-GFP would consist of approximately 4.7×10^8 molecules. The specific interactions between GST and GSH appear to account for more than monolayer coverage of the microspheres based upon the number of GFP molecules that are released.

There are several possible reasons for the multilayer binding to the PEGDA-GSH microspheres. Pendent GSH moieties would be at a distance from the visible surface of the microsphere depending on the length of the growing acrylate backbone before GSH incorporation. Pendant chains extending beyond the surface would greatly increase the amount of protein bound, but not change the apparent size of the particles. GST-GFP could also partially enter the microsphere polymer mesh where the mesh is above the average value. The measured mesh size is based upon the bulk properties and the surface of the microspheres, particularly when loops, entangled loops, and dangling chains are present.

NIH-PA Author Manuscript

NIH-PA Author Manuscript

NIH-PA Author Manuscript

These small changes would be expected to greatly increase the effective surface for binding. Based upon our results, it is clear that multilayers of GST fusion proteins are specifically binding.

To confirm the specificity, a 10 mM GSH solution added to PEGDA-GSH bound GST-GFP resulted in 50% protein elution from the microspheres in 48 hours and complete elution in 6 days (Fig. 4. Low GSH concentrations (below 0.1 μM) in buffered normal saline did not release the protein from the microspheres, further suggesting that the interaction is specific. This is significant since plasma levels are significantly lower at 1.5 μg/mL, or 0.005 mM [43]. Intracellular glutathione concentrations have been measured to be between 1 mM and 10 mM in healthy cells [43], and can be further increased in disease [60, 61]. In the future, we seek to also exploit this characteristic for intracellular release of proteins. In the extracellular environment, the GST-GSH interaction would be expected to be stable for periods of time at low glutathione levels allowing for release specifically in the presence of pathology associated proteases, including thrombin.

Thrombin mediated release of GST fusion proteins is significantly faster than elution with GSH. The velocity of release of GFP was achieved with thrombin concentrations similar to that necessary for clot formation (100 nM, [62]). Association with PEGDA microspheres significantly decreased the rate of thrombin cleavage of GST-GFP (Fig. 5A). This decrease in the enzymatic reaction would be expected to be due to a reduced thrombin affinity for the substrate [63, 64]. In this case, the reduced affinity may be due to unfavorable, rigid or steric limitations of the GST-GFP substrate on the surface of the PEGDA microsphere. Though not further explored in this manuscript, this phenomena may be another modifiable parameter that can allow for more refined control of protein release from immobilized GSH containing hydrogels.

Finally, we showed that GST-melittin could be loaded to the PEGDA-GSH microspheres as efficiently as GST-GFP, and that *S. pyogenes* growth was inhibited by melittin cleaved from PEGDA-GSH microspheres by thrombin. Thrombin is upregulated during bacterial infection, and was, therefore, deemed an appropriate enzyme to be used for activation of anti-bacterial coatings [22]. This would be particularly true for blood-contacting materials. Under these conditions, the melittin released from microspheres was estimated to achieve 1 μM and achieved similar growth inhibition of *S. pyogenes* cells as 1 μM synthetic melittin (Fig. 6). Based upon the growth inhibition, melittin can be loaded predictably on hydrogel microparticles and activated by thrombin. The loaded melittin inhibited growth of high-density cultures of pathogenic *S. pyogenes* cells. These densities of *S. pyogenes* cells would be encountered during active infection, and suggest that the delivery potential of GST-melittin from surface coated material might find further utility as a treatment for active infection.

Bacterial infection coincides with a decrease in pH, and it has been reported that pH values below 6 have been measured in effusions and abscesses caused by bacterial infection [65]. The behavior of an anchor system in these environments would need consideration. The GST/GSH interaction has been shown to be favorable in pH values as low as 5 [66]. In addition, GST and GST-melittin are both stable to denaturation at low pH [23]. It is, therefore, suggested that the GST anchor will maintain anti-bacterial protein immobilized to a surface in low pH environments. We plan to verify the predicted response to decreased pH in the future to fully understand the possibly mechanisms of non-specific release from the microspheres.

Further, even if melittin is not released from the microspheres or if GST-melittin is released there may be non-specific toxicity. During the development of a method to purify proteins

NIH-PA Author Manuscript

NIH-PA Author Manuscript

NIH-PA Author Manuscript

from the insoluble protein fraction, we noted that melittin fused to GST had significantly reduced toxicity [23]. Since this is true, there is already evidence that toxicity would be minimized for the fusion protein. There is some activity, but not statistically different from the control, when microspheres are incubated in the presence of bacteria. Two possible explanations can account for this biological activity: (1) the surface bound melittin is active or (2) melittin is being released from the particles based upon a bacterial mechanism. Unfortunately, our results do not completely eliminate either option. Our observations (unpublished data) suggest that GST-GFP is not released from microspheres in the presence of bacteria by proteolysis in the portion of the molecules that are equivalent or GST-GSH interaction disruption. But, there may be proteolytic activity in the melittin specific portion of the protein.

As a proof of concept for the design of GST-GSH hydrogel protein delivery systems, the fact that activation is necessary for full melittin activity clearly confirms the system functions as designed. In addition, utilization of the GST-GSH interaction as an anchor need not be limited to peptides that show reduced toxicity when they are fused to GST. Proteins or peptides that show activity as fusion proteins may be anchored via a GST/GSH anchor within the hydrogel mesh. Hydrogel mesh size is an easily modifiable parameter [30]. A delivery system that protects protein cargo within a hydrogel mesh would require control of mesh size large enough so that a suitable releasing enzyme, such as thrombin, could enter the hydrogel, cleave the active protein from fused GST, and allow the cleaved product to diffuse out. On the other hand, the mesh size must be small enough to keep therapeutic protein cargo protected from acting before it is release. Future developments of the delivery system will utilize both surface and interior loading of therapeutic proteins that may be designed to allow or minimize activity while loaded.

In conclusion, we have shown that GSH immobilized on the surface of PEGDA microspheres can specifically and predictably interact with GST fused GFP and melittin. The interaction is stable under extracellular salt and GSH conditions. Further, thrombin can release proteins fused to the GST and allow them to exert biologic activity. In our case, melittin was released from the surface and was as functional as melittin at a similar concentration in inhibiting the growth of pathogenic *S. pyogenes*. This proof of concept study established the possibility of using the GST-GSH interaction to load therapeutic proteins into a hydrogel-microsphere-based drug delivery system.

Acknowledgments

This investigation was conducted in a facility constructed with support from Research Facilities Improvement Program Grant (RR15482) from the National Centre for Research Resources of the National Institutes of Health (NIH). This research has been funded, in part, by the University of Illinois at Chicago Center for Clinical and Translational Science (CCTS) award supported by the NCRR (UL1 TR000050, RAG), and the National Institute for Neurologic Disorders and Stroke (NS055095, RAG) and the National Institute of Allergy and Infectious Diseases (AI091779, MJF). The authors also thank Dr. Debra A. Tonetti for use of instruments.

References

1. Haley RW, Hooton TM, et al. Nosocomial infections in U.S. hospitals, 1975–1976: estimated frequency by selected characteristics of patients. Am J Med. 1981; 70:947–959. [PubMed: 6938129]
2. Klevens RM, Edwards JR, et al. Estimating health care-associated infections and deaths in U.S. hospitals, 2002. Public Health Rep. 2007; 122:160–166. [PubMed: 17357358]
3. Wisplinghoff H, Bischoff T, et al. Nosocomial bloodstream infections in US hospitals: analysis of 24,179 cases from a prospective nationwide surveillance study. Clin Infect Dis. 2004; 39:309–317. [PubMed: 15306996]

NIH-PA Author Manuscript

NIH-PA Author Manuscript

NIH-PA Author Manuscript

4. D'Este M, Eglin D. Hydrogels in calcium phosphate moldable and injectable bone substitutes: Sticky excipients or advanced 3-D carriers? Acta Biomater. 2013; 9:5421–5430. [PubMed: 23201020]
5. Nablo BJ, Schoenfisch MH. Antibacterial properties of nitric oxide-releasing sol-gels. J Biomed Mater Res A. 2003; 67:1276–1283. [PubMed: 14624514]
6. Price JS, Tencer AF, et al. Controlled release of antibiotics from coated orthopedic implants. J Biomed Mater Res. 1996; 30:281–286. [PubMed: 8698690]
7. Bologna RA, Tu LM, et al. Hydrogel/silver ion-coated urinary catheter reduces nosocomial urinary tract infection rates in intensive care unit patients: a multicenter study. Urology. 1999; 54:982–987. [PubMed: 10604694]
8. Rojas IA, Slunt JB, Grainger DW. Polyurethane coatings release bioactive antibodies to reduce bacterial adhesion. J Control Release. 2000; 63:175–189. [PubMed: 10640591]
9. Hetrick EM, Schoenfisch MH. Reducing implant-related infections: active release strategies. Chem Soc Rev. 2006; 35:780–789. [PubMed: 16936926]
10. Don TM, Chen CC, et al. Preparation and antibacterial test of chitosan/PAA/PEGDA bi-layer composite membranes. J Biomater Sci Polym Ed. 2005; 16:1503–1519. [PubMed: 16366335]
11. Kong M, Chen XG, et al. Antibacterial mechanism of chitosan microspheres in a solid dispersing system against E. coli. Colloids Surf B Biointerfaces. 2008; 65:197–202. [PubMed: 18508247]
12. Ferraz MP, Mateus AY, et al. Nanohydroxyapatite microspheres as delivery system for antibiotics: release kinetics, antimicrobial activity, and interaction with osteoblasts. J Biomed Mater Res A. 2007; 81:994–1004. [PubMed: 17252559]
13. Tauro JR, Gemeinhart RA. Matrix metalloprotease triggered delivery of cancer chemotherapeutics from hydrogel matrixes. Bioconjug Chem. 2005; 16:1133–1139. [PubMed: 16173790]
14. Rathbone, MJ.; Hadgraft, J.; Roberts, MS. Modified-release drug delivery technology. New York: Marcel Dekker; 2003.
15. Martin, AN.; Sinko, PJ.; Singh, Y. Martin's physical pharmacy and pharmaceutical sciences : physical chemical and biopharmaceutical principles in the pharmaceutical sciences. 6th ed.. Baltimore, MD: Lippincott Williams & Wilkins; 2011.
16. Wang Y, Papadimitrakopoulos F, Burgess DJ. Polymeric "smart" coatings to prevent foreign body response to implantable biosensors. J Control Release. 2013
17. Smith DB, Johnson KS. Single-step purification of polypeptides expressed in Escherichia coli as fusions with glutathione S-transferase. Gene. 1988; 67:31–40. [PubMed: 3047011]
18. Kallberg M, Wang H, et al. Template-based protein structure modeling using the RaptorX web server. Nature protocols. 2012; 7:1511–1522.
19. Habermann E. Bee and wasp venoms. Science. 1972; 177:314–322. [PubMed: 4113805]
20. Habermann E, Jentsch J. Sequence analysis of melittin from tryptic and peptic degradation products. Hoppe Seylers Z Physiol Chem. 1967; 348:37–50. [PubMed: 5592400]
21. van den Bogaart G, Guzman JV, et al. On the mechanism of pore formation by melittin. J Biol Chem. 2008; 283:33854–33857. [PubMed: 18819911]
22. Sun H. The interaction between pathogens and the host coagulation system. Physiology (Bethesda). 2006; 21:281–288. [PubMed: 16868317]
23. Buhrman JS, Cook LC, et al. Active, soluble recombinant melittin purified by extracting insoluble lysate of *Escherichia coli* without denaturation. (submitted).
24. Buhrman JS, Rayahin JE, et al. In-house preparation of hydrogels for batch affinity purification of glutathione S-transferase tagged recombinant proteins. BMC Biotechnol. 2012; 12:63. [PubMed: 22989306]
25. Grote A, Hiller K, et al. JCat: a novel tool to adapt codon usage of a target gene to its potential expression host. Nucleic Acids Res. 2005; 33:W526–W531. [PubMed: 15980527]
26. Franco CL, Price J, West JL. Development and optimization of a dual-photoinitiator, emulsion-based technique for rapid generation of cell-laden hydrogel microspheres. Acta Biomater. 2011; 7:3267–3276. [PubMed: 21704198]
27. Davis HW, Sauter RW. Fluorescence of Trypan blue in frozen-dried embryos of the rat. Histochemistry. 1977; 54:177–189. [PubMed: 604320]

NIH-PA Author Manuscript

NIH-PA Author Manuscript

NIH-PA Author Manuscript

28. Yeh J, Ling Y, et al. Micromolding of shape-controlled, harvestable cell-laden hydrogels. Biomaterials. 2006; 27:5391–5398. [PubMed: 16828863]
29. Harrisson F, Callebaut M, Vakaet L. Microspectrographic analysis of trypan blue-induced fluorescence in oocytes of the Japanese quail. Histochemistry. 1981; 72:563–578. [PubMed: 7298390]
30. Ross AE, Tang MY, Gemeinhart RA. Effects of molecular weight and loading on matrix metalloproteinase-2 mediated release from poly(ethylene glycol) diacrylate hydrogels. AAPS J. 2012; 14:482–490. [PubMed: 22535508]
31. Brannon-Peppas, L. Preparation and Characterization of crosslinked hydrophilic networks. In: Brannon-Peppas, L.; Harland, RS., editors. Absorbent Polymer Technology. Amesterdam: Elsevier; 1990. p. 45-65.
32. Hughes SW. Archimedes revisited: a faster, better, cheaper method of accurately measuring the volume of small objects. Phys Educ. 2005; 40:468–474.
33. Peppas NA, Bures P, et al. Hydrogels in pharmaceutical formulations. Eur J Pharm Biopharm. 2000; 50:27–46. [PubMed: 10840191]
34. Bradford MM. A rapid and sensitive method for the quantitation of microgram quantities of protein utilizing the principle of protein-dye binding. Anal Biochem. 1976; 72:248–254. [PubMed: 942051]
35. Maniatis, T.; Fritsch, EF.; Sambrook, J. Molecular cloning : a laboratory manual. Cold Spring Harbor, N.Y.: Cold Spring Harbor Laboratory; 1982.
36. Laemmli UK. Cleavage of structural proteins during the assembly of the head of bacteriophage T4. Nature. 1970; 227:680–685. [PubMed: 5432063]
37. van de Rijn I, Kessler RE. Growth characteristics of group A streptococci in a new chemically defined medium. Infect Immun. 1980; 27:444–448. [PubMed: 6991416]
38. Lim K, Ho JX, et al. Three-dimensional structure of Schistosoma japonicum glutathione S-transferase fused with a six-amino acid conserved neutralizing epitope of gp41 from HIV. Protein Sci. 1994; 3:2233–2244. [PubMed: 7538846]
39. Fabrini R, De Luca A, et al. Monomer-dimer equilibrium in glutathione transferases: a critical re-examination. Biochemistry. 2009; 48:10473–10482. [PubMed: 19795889]
40. Andujar-Sanchez M, Smith AW, et al. Crystallographic and thermodynamic analysis of the binding of S-octylglutathione to the Tyr 7 to Phe mutant of glutathione S-transferase from Schistosoma japonicum. Biochemistry. 2005; 44:1174–1183. [PubMed: 15667211]
41. Yang F, Moss LG, Phillips GN Jr. The molecular structure of green fluorescent protein. Nat Biotechnol. 1996; 14:1246–1251. [PubMed: 9631087]
42. Hubbell JA. Biomaterials in tissue engineering. Bio/Technology. 1995; 13:565–576. [PubMed: 9634795]
43. Tietze F. Enzymic method for quantitative determination of nanogram amounts of total and oxidized glutathione: applications to mammalian blood and other tissues. Anal Biochem. 1969; 27:502–522. [PubMed: 4388022]
44. Graminski GF, Kubo Y, Armstrong RN. Spectroscopic and kinetic evidence for the thiolate anion of glutathione at the active site of glutathione S-transferase. Biochemistry. 1989; 28:3562–3568. [PubMed: 2742854]
45. Chatterjee MS, Denney WS, et al. Systems biology of coagulation initiation: kinetics of thrombin generation in resting and activated human blood. PLoS Comput Biol. 2010; 6
46. Kessels H, Beguin S, et al. Measurement of thrombin generation in whole blood--the effect of heparin and aspirin. Thromb Haemost. 1994; 72:78–83. [PubMed: 7974380]
47. Teitel JM, Bauer KA, et al. Studies of the prothrombin activation pathway utilizing radioimmunoassays for the F2/F1 + 2 fragment and thrombin--antithrombin complex. Blood. 1982; 59:1086–1097. [PubMed: 7074214]
48. Harris, JM. Poly(ethylene glycol) chemistry : biotechnical and biomedical applications. New York: Plenum Press; 1992.
49. Kawaguchi H, Fujimoto K, et al. Modification and functionalization of hydrogel microspheres. Colloid Surf. A-Physicochem. Eng. Asp. 1996; 109:147–154.

NIH-PA Author Manuscript

NIH-PA Author Manuscript

NIH-PA Author Manuscript

50. Behravesh E, Sikavitsas VI, Mikos AG. Quantification of ligand surface concentration of bulk-modified biomimetic hydrogels. Biomaterials. 2003; 24:4365–4374. [PubMed: 12922149]
51. DeLong SA, Moon JJ, West JL. Covalently immobilized gradients of bFGF on hydrogel scaffolds for directed cell migration. Biomaterials. 2005; 26:3227–3234. [PubMed: 15603817]
52. Plunkett KN, Chatterjee AN, et al. Surface-modified hydrogels for chemoselective bioconjugation. Macromolecules. 2003; 36:8846–8852.
53. Shu XZ, Ghosh K, et al. Attachment and spreading of fibroblasts on an RGD peptidemodified injectable hyaluronan hydrogel. J. Biomed. Mater. Res. Part A. 2004; 68A:365–375.
54. Kang CE, Gemeinhart EJ, Gemeinhart RA. Cellular Alignment by Grafted Adhesion Peptide Surface Density Gradients. J. Biomed. Mater. Res. 2004; 71:403–411.
55. Salinas CN, Anseth KS. Mixed Mode Thiol-Acrylate Photopolymerizations for the Synthesis of PEG-Peptide Hydrogels. Macromolecules. 2008; 41:6019–6026.
56. Nichols MD, Scott EA, Elbert DL. Factors affecting size and swelling of poly(ethylene glycol) microspheres formed in aqueous sodium sulfate solutions without surfactants. Biomaterials. 2009; 30:5283–5291. [PubMed: 19615738]
57. Scott EA, Nichols MD, et al. Modular scaffolds assembled around living cells using poly(ethylene glycol) microspheres with macroporation via a non-cytotoxic porogen. Acta Biomaterialia. 2010; 6:29–38. [PubMed: 19607945]
58. Yan X, Gemeinhart RA. Cisplatin delivery from poly(acrylic acid-co-methyl methacrylate) microparticles. J. Control. Release. 2005; 106:198–208. [PubMed: 15979187]
59. Zhang Y, Gemeinhart RA. Improving Matrix Metalloproteinase-2 Specific Response of a Hydrogel System using Electrophoresis. Int. J. Pharm. 2012; 429:31–37. [PubMed: 22440150]
60. Godwin AK, Meister A, et al. High resistance to cisplatin in human ovarian cancer cell lines is associated with marked increase of glutathione synthesis. Proc Natl Acad Sci U S A. 1992; 89:3070–3074. [PubMed: 1348364]
61. Lewis AD, Hayes JD, Wolf CR. Glutathione and glutathione-dependent enzymes in ovarian adenocarcinoma cell lines derived from a patient before and after the onset of drug resistance: intrinsic differences and cell cycle effects. Carcinogenesis. 1988; 9:1283–1287. [PubMed: 2898306]
62. Dashkevich NM, Ovanesov MV, et al. Thrombin activity propagates in space during blood coagulation as an excitation wave. Biophys J. 2012; 103:2233–2240. [PubMed: 23200057]
63. Copeland, RA. Enzymes : a practical introduction to structure, mechanism, and data analysis. 2nd ed.. New York: Wiley; 2000.
64. Briggs GE, Haldane JB. A Note on the Kinetics of Enzyme Action. Biochem J. 1925; 19:338–339. [PubMed: 16743508]
65. Simmen HP, Blaser J. Analysis of pH and pO2 in abscesses, peritoneal fluid, and drainage fluid in the presence or absence of bacterial infection during and after abdominal surgery. Am J Surg. 1993; 166:24–27. [PubMed: 8328625]
66. Ortiz-Salmeron E, Yassin Z, et al. Thermodynamic analysis of the binding of glutathione to glutathione S-transferase over a range of temperatures. Eur J Biochem. 2001; 268:4307–4314. [PubMed: 11488926]

NIH-PA Author Manuscript
NIH-PA Author Manuscript
NIH-PA Author Manuscript

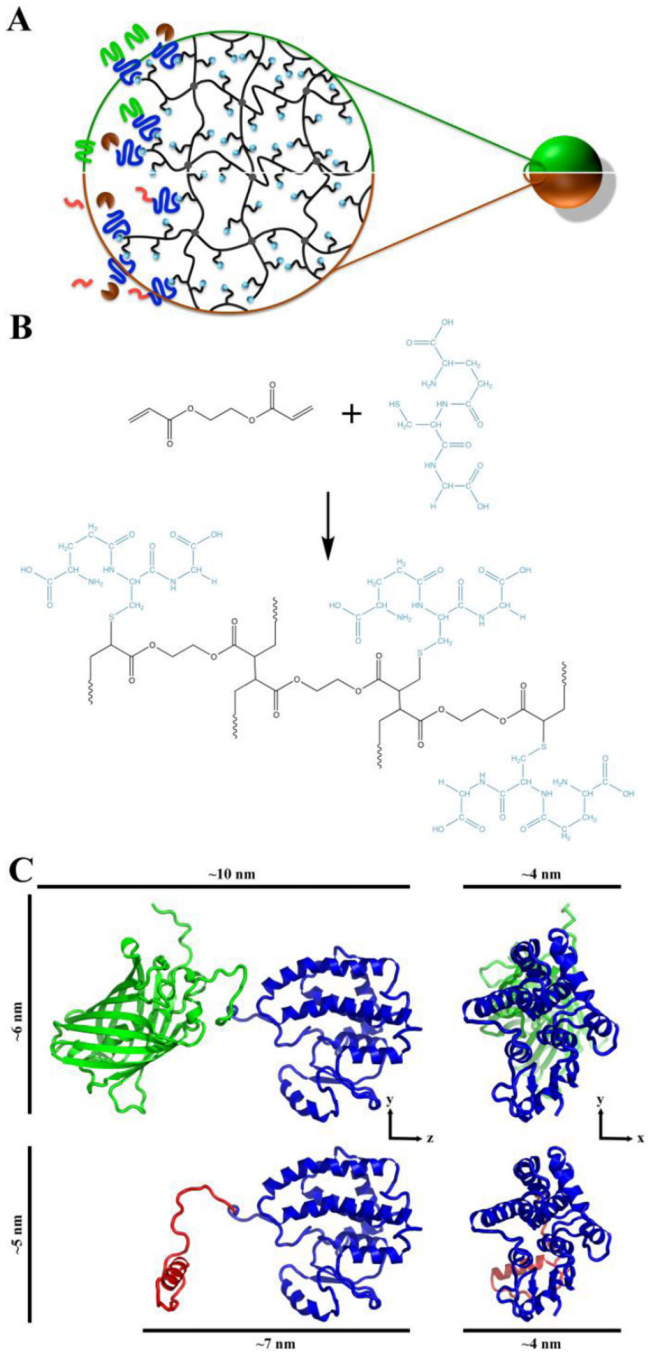

Fig. 1. Schematic of PEGDA-GSH microspheres and predicted structure of GST-GFP and GST-melittin

(A) Schematic showing half of a GST-GFP (green/top) and half of a GST-melittin (orange/bottom) microsphere with a magnified region of the microspheres suggesting the surface and internal structure. In the magnified region, black entanglements indicate the crosslinked (grey circles) PEGDA mesh with pendant glutathione (GSH; gold spheres). GST (blue)-GFP (green) and GST-melittin (pink) fusion protein are shown binding to GSH. Thrombin (brown) is shown cleaving melittin or GFP from GST fusion partners by acting on a thrombin cleavage site in linker fragment. (B) Schematic of the chemical structure of the PEGDA-GSH hydrogel. (C) Predicted three-dimensional structures of GST (blue)-GFP

(green) fusion protein and GST (blue)-melittin (red) fusion protein monomers [18] used to estimate the size of the fusion proteins. Distances are approximations of the longest three dimensions of the fusion proteins.

NIH-PA Author Manuscript
NIH-PA Author Manuscript
NIH-PA Author Manuscript

NIH-PA Author Manuscript
NIH-PA Author Manuscript
NIH-PA Author Manuscript

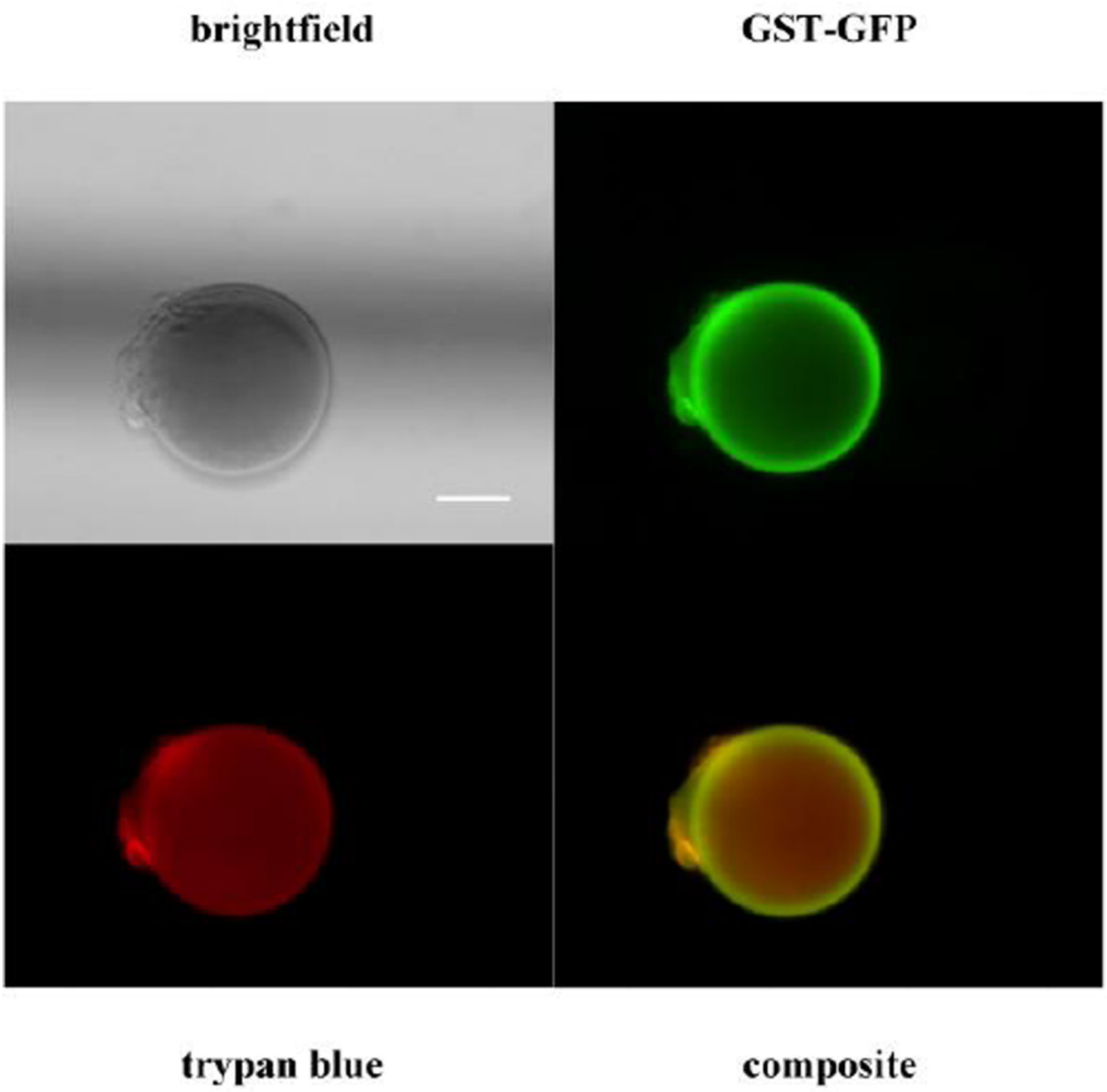

Fig. 2. Binding of GST-GFP to PEGDA-GSH microspheres

Brightfield (upper left) and pseudo-color composite micrograph (lower right) of GST-GFP (green/upper right) bound to GST-PEGDA microspheres counterstained with trypan blue (red/lower left). The scale bar is 10 μm.

NIH-PA Author Manuscript
NIH-PA Author Manuscript
NIH-PA Author Manuscript

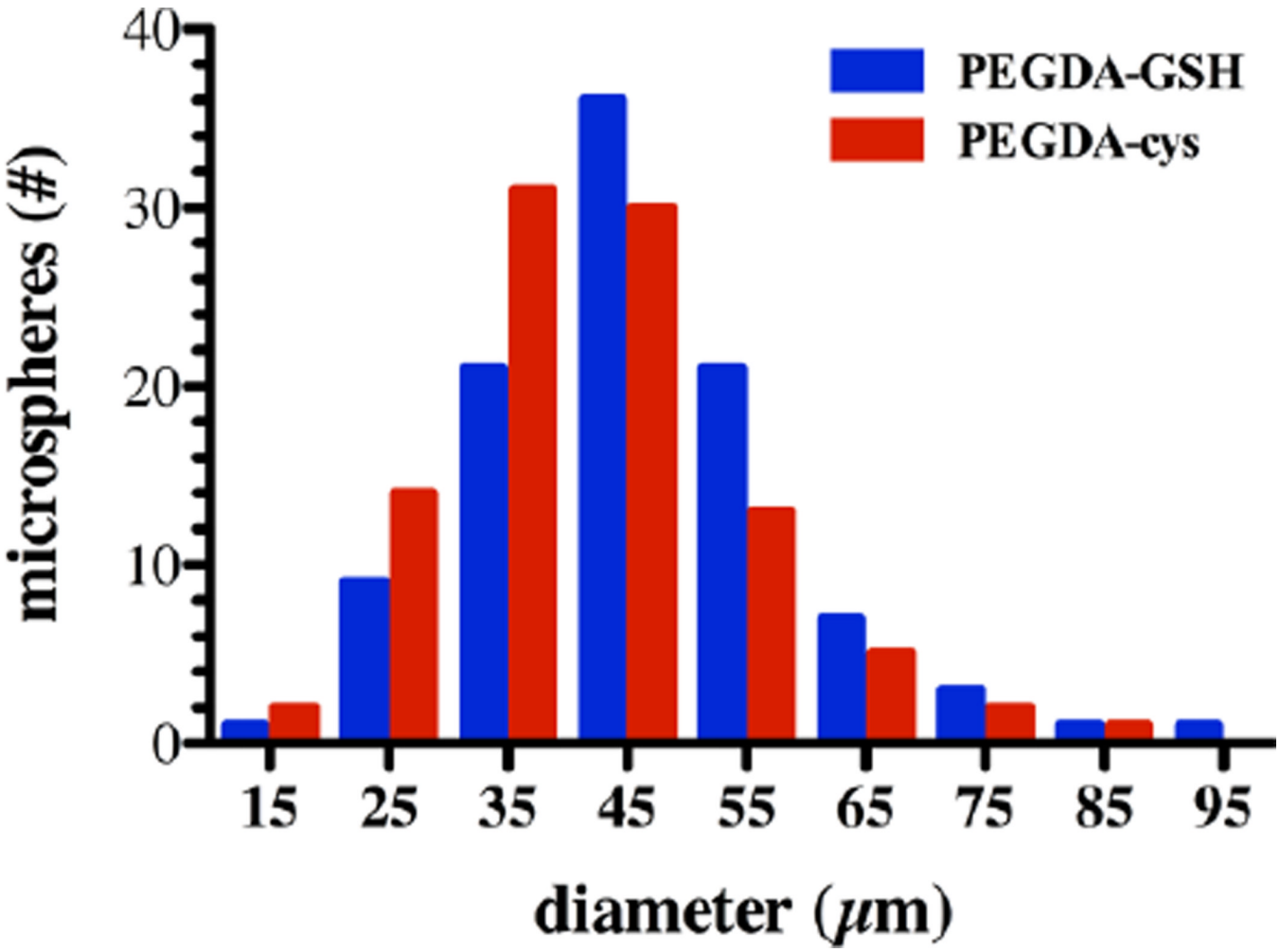

Fig. 3. Size Distribution of PEGDA-GSH and PEGDA-cys microspheres

Representative histogram showing the diameters of PEGDA-GSH (blue) and PEGDA-cys (red) microspheres from a single production batch. Three batches were used to calculate average microsphere diameter and are presented in Table 2.

NIH-PA Author Manuscript

NIH-PA Author Manuscript

NIH-PA Author Manuscript

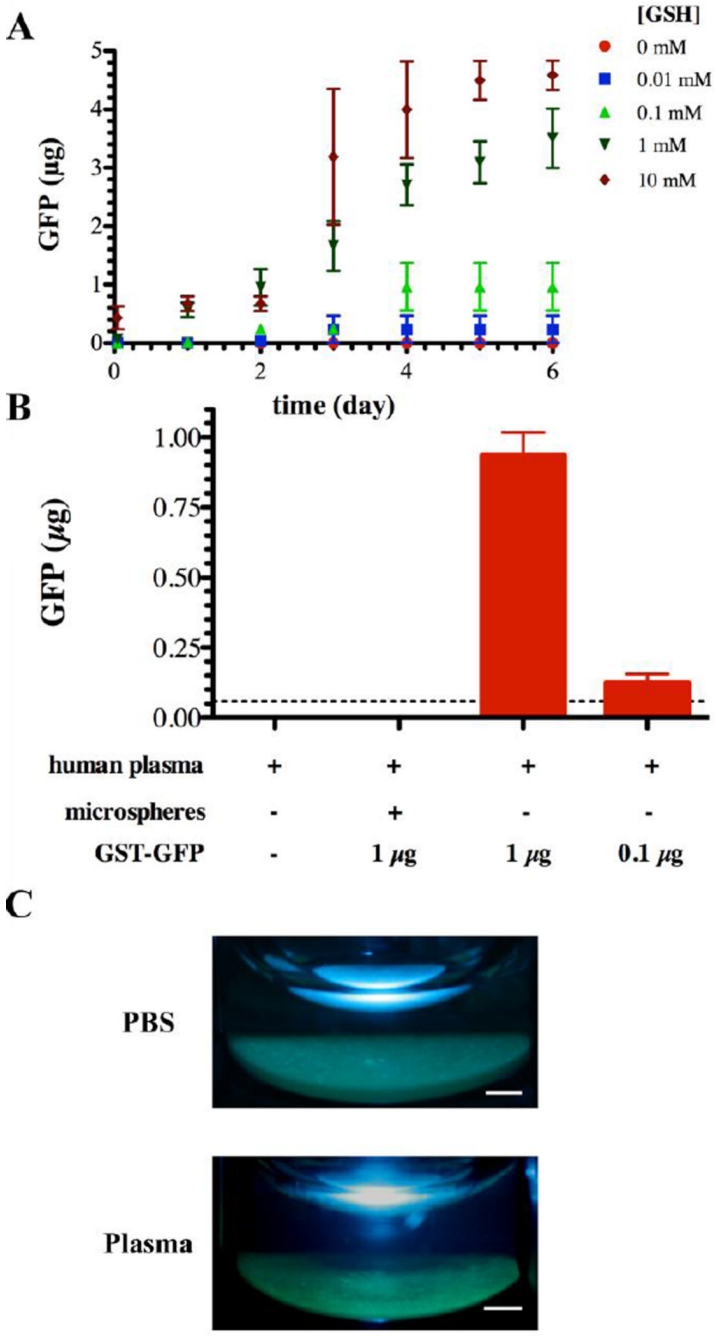

Fig. 4. Release of GST-GFP in the presence of biologic fluids

(**A**) Release of GST-GFP in the presence of 10 mM (♦), 1 mM (▼), 0.1 mM (▲), 0.01 mM (■), and 0 mM (●) GSH containing phosphate buffered saline. Each point represents the mean plus or minus the standard deviation of three independent samples. (**B**) Human plasma mediated release of GFP from GST-GFP loaded PEGDA-GSH microspheres. Microspheres were incubated with human plasma for 6 days at 37°C prior to measuring GFP in the supernatant by fluorescence. Each point represents the mean plus or minus the standard error of the mean of three independent samples in plasma from 3 human donors. (**C**) Gross

photographs of microspheres under UV illumination after 6 days of incubation in human plasma or PBS at 37°C. The scale bar is 1 mm.

NIH-PA Author Manuscript
NIH-PA Author Manuscript
NIH-PA Author Manuscript

NIH-PA Author Manuscript
NIH-PA Author Manuscript
NIH-PA Author Manuscript

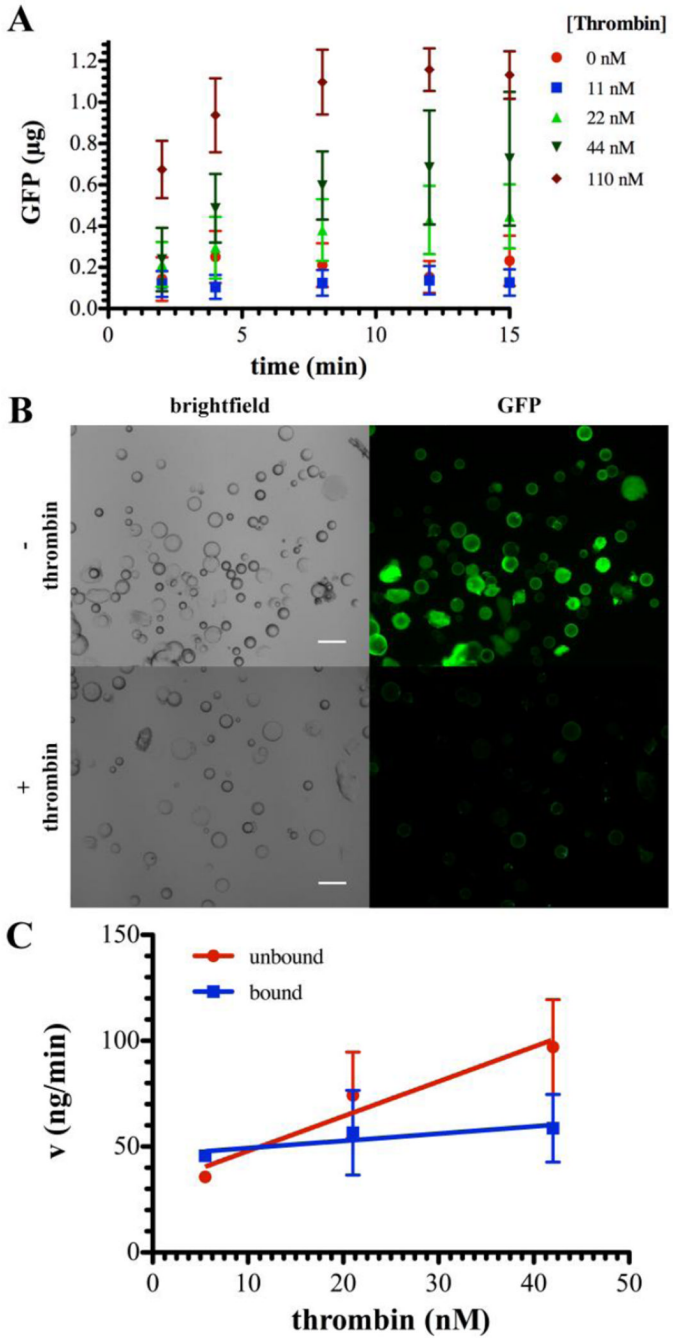

Fig. 5. Thrombin cleavage of GST-GFP from with PEGDA microspheres

(A) Release of GFP from GST-GFP PEGD-GSH microspheres in the presence of (●) 0, 11 (■), 22 (▼), 44 (▲), or 110 (◆) nM thrombin as detected by fluorescent GFP signal. Each point represents the mean plus or minus the standard deviation of three independent samples. **(B)** Representative brightfield and epifluorescent micrographs depicting GST-GFP (green) associated with microspheres before (top row) or after (bottom row) release in response to thrombin (1.8 μM). (**C**) Rate (v) of GFP liberation from GST-GFP (unbound; ■) and GST-GFP (bound; ●) bound to PEGDA-GSH microspheres for the linear portion of the

rate curve, typically the first 1 hour. Each point represents the mean plus or minus the standard deviation of three independent samples.

NIH-PA Author Manuscript
NIH-PA Author Manuscript
NIH-PA Author Manuscript

NIH-PA Author Manuscript

NIH-PA Author Manuscript

NIH-PA Author Manuscript

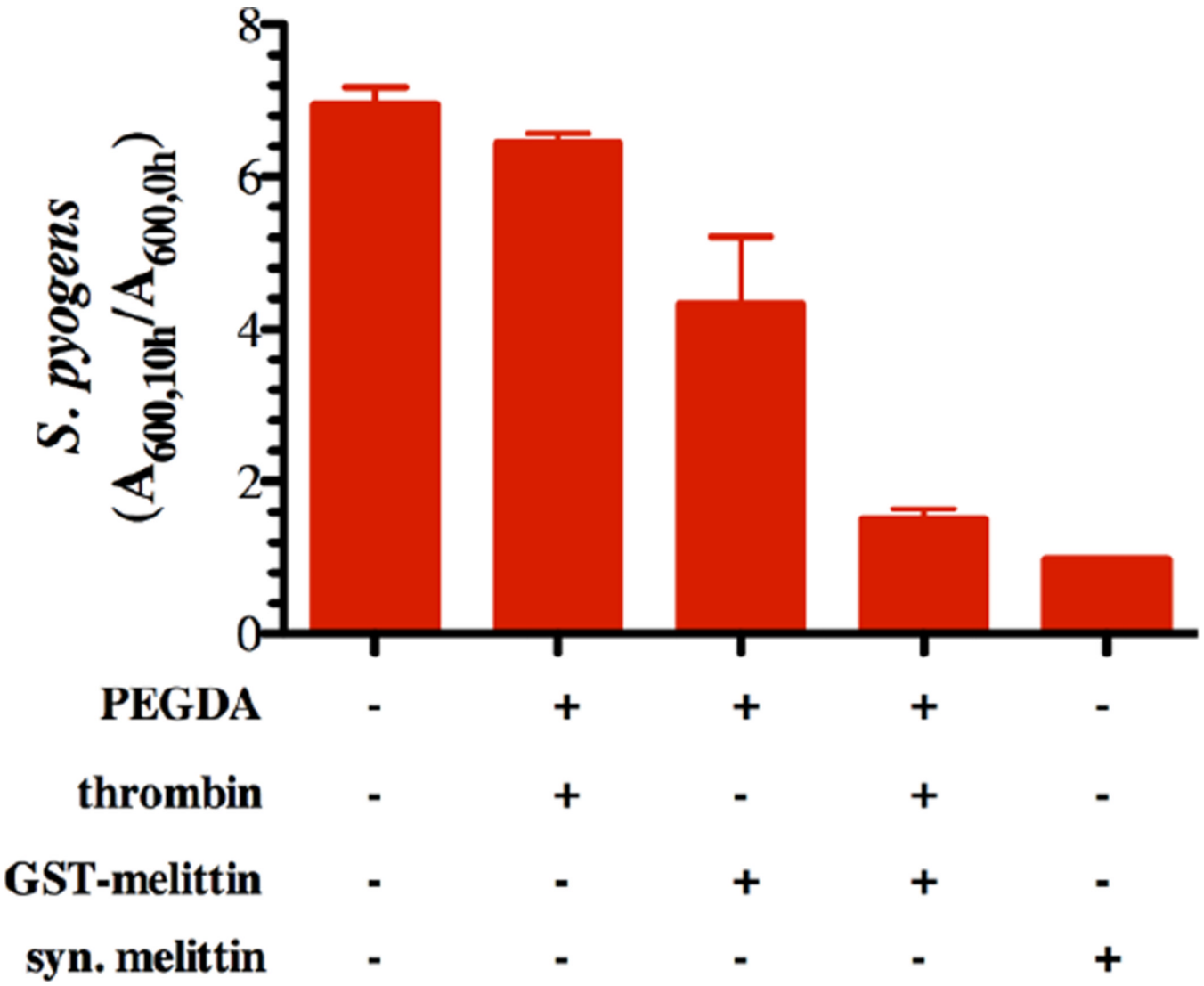

Fig. 6. GST-melittin microspheres inhibit growth of *S. pyogenes*

Growth inhibition of *S. pyogenes* cells exposed for 10 hours to chemically defined growth medium (CDM), CDM with synthetic melittin (syn. Melittin), or CDM mixed with the releasate from PEGDA-GSH microspheres with thrombin, PEGDA-GSH microspheres bound with GST-melittin, or PEGDA-GSH microspheres bound with GST-melittin and exposed to thrombin (1.8 μM) for 2 hours. The data is presented as the absorbance at 600 nm following 10 hours of growth divided by the absorbance at 600 nm following 1 hour of growth. Each bar represents the mean plus or minus the standard error of the mean of three to four technical replicates.

NIH-PA Author Manuscript

NIH-PA Author Manuscript

NIH-PA Author Manuscript

Table 1

Calculated dimensions of GST and GST fusion proteins.

Protein	x * y * z (nm × nm × nm)[§]	
	Monomer	Dimer
GST[†]	4 × 4.5 × 9	5 × 9 × 9
GST-GFP[‡]	4 × 6 × 10	8 × 10 × 10
GST-melittin[‡]	4 × 5 × 7	8 × 10 × 7

[†]Based upon published crystal structures for the dimer [38, 39] and MacPyMol [42] measurement of a single monomer from the dimer crystal structure.

[‡]Measured in MacPyMol [42] from Raptor X structure prediction and alignment of the GST-GST dimer [18].

[§]x, y, and z lengths of the protein using arbitrary coordinates similar to those represented in Figure 1.

NIH-PA Author Manuscript

NIH-PA Author Manuscript

NIH-PA Author Manuscript

Table 2

Summary of physical parameters of PEGDA-GSH microspheres.

Parameter		Calculated Value	Observed Value
Particle	Diameter (μm)	-	46±16
	Surface Area (μm^2)	-	6,647±804
	Mesh Size (nm)	-	4.6±0.2
GST-GFP	Cross Sectional Area[†] (μm^2/molecule)	1.4×10^{-5}	-
	Capacity[§‡] (molecule/microsphere)	4.7×10^{8}	$9.9\pm2.5\times10^{8}$

[†]Estimated based upon the crystal structure of a GST dimer and predicted structure of the fusion proteins.

[§]Estimated from the observed microsphere diameter and estimated cross sectional area of GST-GFP.

[‡]Observed value was determined from thrombin release from microspheres.